analytical chemistry

pubs.acs.org/ac Article

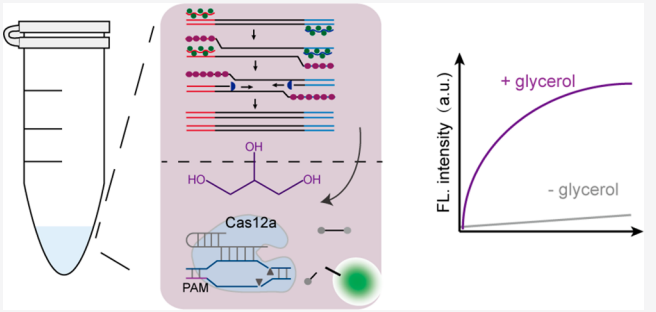
Glycerol Additive Boosts 100-fold Sensitivity Enhancement for One-Pot RPA-CRISPR/Cas12a Assay

Mei Lin, Huahua Yue, Tian Tian, Erhu Xiong, Debin Zhu, Yongzhong Jiang,* and Xiaoming Zhou*

Cite This: *Anal. Chem.* 2022, 94, 8277−8284 Read Online

ACCESS | Metrics & More | Article Recommendations | Supporting Information

ABSTRACT: CRISPR/Cas12, a highly efficient and specific nucleic acid recognition system, has been broadly employed to detect amplified DNA products. However, most reported methods adopt a two-step detection mode that needs a liquid transfer step, thus complicating the detection procedure and posing a risk of aerosol contamination. A one-pot detection method can obviate these problems, but it suffers from poor detection efficiency due to the loss of amplification templates elicited by CRISPR/Cas12 cleavage. In this study, we discovered that a glycerol additive dramatically promoted the detection efficiency of the one-pot recombinase polymerase amplification (RPA)-CRISPR/Cas12a method. Compared with the glycerol-free version, its sensitivity was nearly 100-fold higher and was close to that of the canonical two-step method. Further investigation displayed that the enhanced detection efficiency was attributed to the phase separation of the RPA and CRISPR/Cas12a system during the initial phase of the RPA reaction caused by the glycerol viscosity. This highly efficient one-pot method has been triumphantly harnessed for the detection of African swine fever virus (ASFV) and SARS-CoV-2, achieving naked-eye readout through a smartphone-equipped device. The currently developed glycerol-enhanced one-pot RPA-CRISPR/Cas12a method can be an advantageous point-of-care nucleic acid detection platform on account of its simplicity, high sensitivity, and universality.



Downloaded via SHANGHAI NORMAL UNIV on February 18, 2025 at 06:03:49 (UTC).
See https://pubs.acs.org/sharingguidelines for options on how to legitimately share published articles.

INTRODUCTION

Owing to their rapidity, accuracy, high sensitivity, and specificity, nucleic acid based diagnostic methods have recently emerged as the predominant diagnostic methods for infectious diseases, agriculture, food safety, and environmental monitoring.[1−3] In recent years, CRISPR (cluster regularly interspaced short palindromic repeats)/Cas (CRISPR-associated) systems have developed rapidly because of their high sensitivity, specificity, programmability, and ease of use, and they have exhibited a promising preponderance for gene editing and diagnosis applications.[4−6] Especially some common Cas nucleases, such as Cas12a, Cas12b, Cas12f, and Cas13a, which present amplified collateral cleavage mechanisms, can indiscriminately degrade nonspecific single-stranded nucleic acids after target recognition.[7−11] On account of this unique characteristic, the developed emerging CRISPR/Cas-based assay was deemed to be a prevailing nucleic acid testing method, promoting the rapid evolution of next-generation molecular diagnostic platforms.[12,13]

Although CRISPR-based tools take on powerful and robust signal amplification peculiarity, their detection ability is still not enough for directly measure clinical samples without nucleic acid amplification.[14,15] To further boost the detection sensitivity of this system, CRISPR technology is usually combined with nucleic acid amplification technology.[16] In particular, when a CRISPR/Cas system was integrated with LAMP (loop-mediated isothermal amplification),[17] RPA (recombinase polymerase amplification),[18] and other isothermal amplification technologies, nucleic acid detection displayed the features of ease of use, quick turnaround time, and field test capacity.[19,20] Some early developed nucleic acid amplification based CRISRP detection methods, such as the SHERLOCK (Specific High-sensitivity Enzymatic Reporter UnLOCKing) technology based on Cas13 nuclease and the DETECTR (DNA Endonuclease-Targeted CRISPR Trans Reporter) and HOLMES (one-Hour Low-cost Multipurpose highly Efficient System) technologies based on Cas12 nuclease,[8,21−23] usually contained two separate procedures: nucleic acid amplification and CRISPR end point detection. Nonetheless, in these assays, the testing procedure needs the transfer of amplified products, which easily causes aerosol contamination thus leading to false positive risk. To address the above issues, some one-pot methods integrating nucleic acid amplification and CRISPR detection into a single reaction

Received: February 6, 2022
Accepted: May 16, 2022
Published: May 30, 2022



ACS Publications © 2022 American Chemical Society

https://doi.org/10.1021/acs.analchem.2c00616
Anal. Chem. 2022, 94, 8277−8284

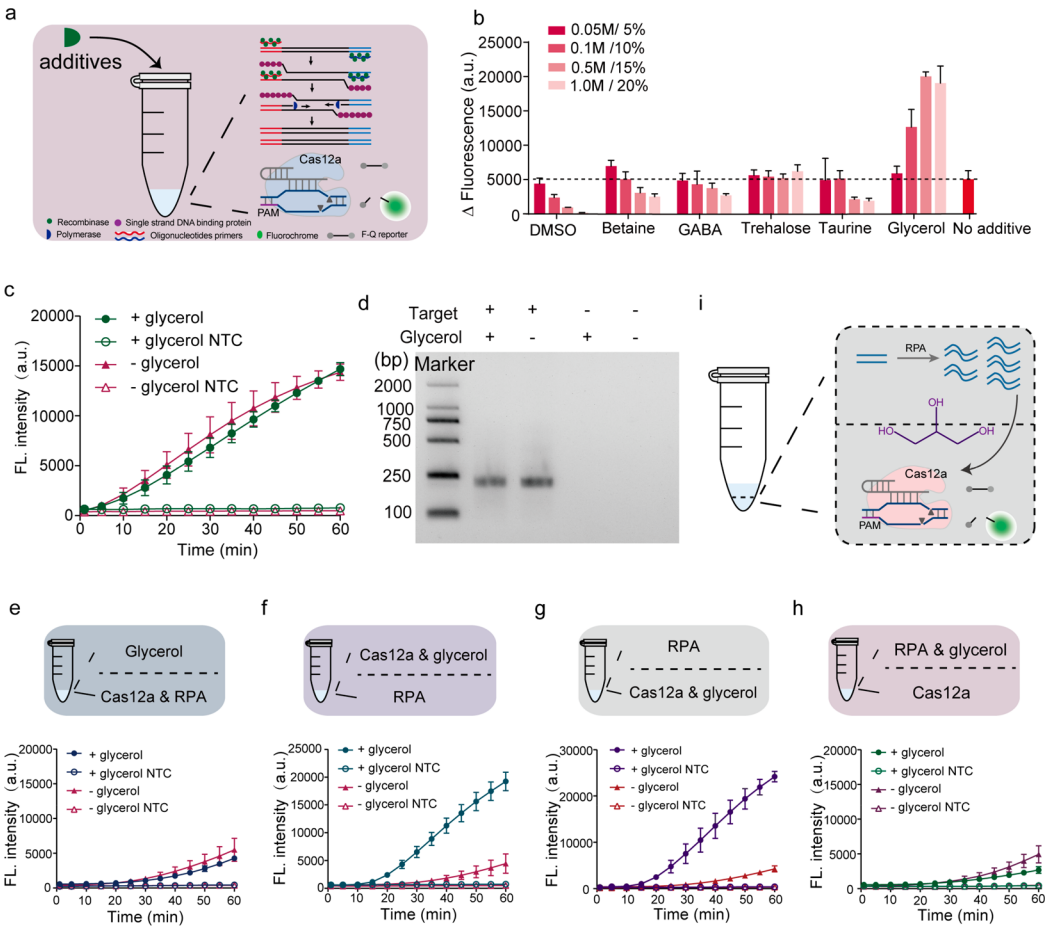


Figure 1. Establishment of glycerol-enhanced one-pot RPA-CRISPR/Cas12a method. (a) Schematic illustration of additives acting on one-pot RPA-CRISPR/Cas12a. (b) Evaluation of the effects of different additives on one-pot RPA-CRISPR/Cas12a. (c) Assessment of the effects of 15% glycerol on CRISPR/Cas12a system. (d) Gel electrophoresis analysis of the effects of 15% glycerol on RPA reaction. (e) Corresponding to experiences i, where the mixtures of RPA and CRISPR system were on the bottom of tube and the glycerol was on top. (f) Corresponding to experiences ii, where the RPA component was on the bottom and the mixtures of glycerol and CRISPR system were on top. (g) Corresponding to experiences iii, where the mixtures of glycerol and CRISPR system were on the bottom of the tube and the RPA was on top. (h) Corresponding to experiences iv, where the CRISPR system was on the bottom of the tube and the mixtures of RPA and glycerol were on top. The schematic diagram is shown above, and the fluorescence curve is shown below. (i) Schematic of glycerol-enhanced one-pot RPA-CRISPR/Cas12a method. Error bars represent the mean ± standard deviation (SD) from three replicates. NTC represents no target control.

system, such as SHERLOCKv2 and HOLMESv2, have been exploited.[24,25] These methods are simpler and circumvent the risk of uncapping contamination induced by amplification product transfer but generally suffer from poor sensitivity. For example, the one-pot method based on the combination of CRISPR/Cas12 and RPA was heavily less sensitive than the two-step detection strategy.[8] This problem is elicited by the following: (i) CRISPR/Cas12a is capable of recognizing and degrading amplification template DNA efficiently on the basis of its cis-cleavage activity under the guidance of crRNA.[26] The cleavage site locates into the amplification region of RPA; hence the DNA template of RPA will be lost at the initial stage of amplification compromising one-pot detection efficiency. (ii) Trans-cleavage activity triggered by CRISPR/Cas12a upon specific target recognition would nonspecifically degrade single-strand primers of RPA in the system,[7,8] thus whittling down the efficiency of RPA isothermal amplification. Therefore, to elevate the sensitivity of the one-pot method, it should try its best to avert mutual interference between the CRISPR system and isothermal amplification in the tube.

Recently, a few attempts have been devoted to ameliorating the aforementioned issues. For example, some physical strategies including adding Cas12a kits to the wall or cap of the tube,[27−29] taking advantage of the density difference of sucrose concentrations,[30] and employing microfluidic technology[31,32] were executed to spatially separate the CRISPR system and isothermal amplification in the tube and microchannel. However, there are still some restrictions in these studies, such as the demand for additional centrifugation steps, or limited sensitivity, or high cost. It is also demonstrated that reducing the dosage of Cas12a can minimize the interference on RPA amplification, but at the cost of inferior sensitivity and longer response time.[33] In another study, researchers introduced the dual crRNA without PAM (protospacer adjacent motif) site limitation to fulfill highly sensitive one-pot SARS-CoV-2 detection, but its generality is still unproven.[34] That is, at present, it remains an unmet demand to develop a one-pot RPA-CRISPR/Cas12a nucleic acid assay method with high sensitivity, usability, and universality.

In this study, we propose a simple and cost-efficient solution for this project. In this method, an efficient one-pot RPA-

https://doi.org/10.1021/acs.analchem.2c00616
Anal. Chem. 2022, 94, 8277−8284

CRISPR/Cas12a method can be achieved by simply adding glycerol to the system. Compared with the ordinary glycerol-free one-pot detection method, its sensitivity boosted by nearly 2 orders of magnitude and was close to the sensitivity (aM) of the canonical two-step method. Moreover, in this assay all the components of RPA amplification and CRISPR detection were simultaneously placed in a single one-pot reaction system and incubated at 37 °C, dispelling the requirement for separate preamplification and transfer of amplification products. Meanwhile, results can be detected directly by the naked eye via constructing a portable fluorescent detection device. This method exhibited excellent versatility and has been resoundingly leveraged to detect SARS-CoV-2 and African swine fever virus (ASFV) with high sensitivity and specificity. In brief, we propose a universal, easy-to-use, ultrasensitive, and laboratory infrastructure-independent one-pot nucleic acid detection platform, presenting great promise for rapid, accurate point-of-care (POC) testing.

EXPERIMENTAL SECTION

Glycerol-Enhanced One-Pot RPA-CRISPR/Cas12a Analysis. The one-pot system was prepared separately as components A and B. Component A contained 1 × 2.1 NEBuffer, 100 nM LbCas12a, 100 nM crRNA, 400 nM FQ probe, and 15% glycerol. Component B is the RPA system and included 29.5 μL of primer-free rehydration buffer, 240 nM forward and reverse primers, one freeze-dried reaction pellet, target, and RNase-free water. The concentration in each component was calculated on the basis of the finally assembled 20 μL one-pot system. In the one-pot assay, 10 μL of component A was added into the bottom of the tube, 9.5 μL of component B was added into the tube well, and finally 0.5 μL of 280 mM magnesium acetate was added; then brief centrifugation took place before real-time fluorescence monitoring. For one-pot RT-RPA-CRISPR/Cas12a assays, most components were the same as those in the one-pot system, except for supplementation with 0.5 μL of SuperScript IV reverse transcriptase (200 U/μL) and 1 μL of RNase H[35] (5 U/μL) in component B. All the reactions were carried out at 37 °C for 60 min. Real-time fluorescence signals were recorded every minute. Visual detection was accomplished through imaging the tubes in the readout device.

For additional experimental details, please refer to the Supporting Information.

RESULTS AND DISCUSSION

Glycerol-Enhanced One-Pot RPA-CRISPR/Cas12a Method. Previous studies have indicated that some additives could enhance the efficiency of nucleic acid detection. For example, betaine, dimethyl sulfoxide (DMSO), glycerol, γ-aminobutyric acid (GABA), and trehalose have been shown to accelerate polymerase chain reaction (PCR) or isothermal amplification.[36−39] Recent studies have also demonstrated that betaine, DMSO, and glycerol promote the efficiency of CRISPR detection.[39,40] Considering the poor sensitivity of the conventional one-pot RPA-CRISPR detection system, here we seek to screen some additives that can improve the detection efficiency. In this study, we evaluated the effects of six additives (DMSO, betaine, GABA, trehalose, taurine, and glycerol) on the one-pot RPA-CRISPR reaction system (Figure 1a). Excitingly, we found that glycerol presented a significant enhancement in detection efficiency. Further observation elucidated that the enhancement was dependent on the glycerol concentration and the enhancement effect was optimal at 15% glycerol (Figure 1b).

Next, the mechanism of glycerol enhancing the one-pot RPA-CRISPR/Cas12a system was investigated. We conjectured that the promotion in detection efficiency might be ascribed to how glycerol enhanced the RPA reaction or CRISPR detection. Whereupon the influence of glycerol on the CRISPR system was first questioned via an independent CRISPR/Cas12a assay, and the result explicated that glycerol was unable to promote the CRISPR reaction (Figure 1c). Then, we also examined the effect of glycerol on RPA amplification through gel electrophoresis analysis. Unexpectedly, the electrophoretic bands revealed that the RPA amplification reaction was slightly inhibited by the glycerol (Figure 1d). Meanwhile, a similar result was acquired by adopting the CRISPR/Cas12a system to detect the amplification products (Figure S1).

Since glycerol exerted no positive impact on either the RPA or CRISPR reaction system, the notable promotion in detection efficiency of the one-pot system may not be on account of its chemical properties but because of a physical property: viscosity. In our one-pot experiment, the mixtures of glycerol and CRISPR system were first placed at the bottom of the tube, then the RPA component was added to the tube wall, and finally centrifugation took place. That is, the CRISPR system and RPA system were not mixed directly. Furthermore, it was found that glycerol had no positive effect on the one-pot assay when the CRISPR system and RPA reagents were completely mixed (Figure S2). Hence, we surmised that viscous glycerol played its part in separating the CRISPR system from the RPA system at the initial stage of RPA amplification in the one-pot reaction, which delayed the fusion of the Cas12a detection system and RPA amplification in the tube. Also, the RPA amplification in one pot was scarcely compromised by the CRISPR system, thereby tremendously stimulating one-pot assay efficiency. Subsequently, we changed the position of three components in the tube and carried out four experiments to validate this hypothesis. In experiment i, where the CRISPR/Cas12 system and the RPA system were not separated by glycerol, it was illuminated that glycerol had no facilitation for the detection efficiency of the one-pot reaction (Figure 1e). Differently, in experiments ii and iii, there was glycerol separating the CRISPR system from the RPA system in the tube and the assay efficiency of the one-pot system was strikingly boosted upon the addition of glycerol (Figure 1f,g). In experiment iv, although the RPA components and CRISRP system were not mixed, the fluorescence signal was slightly attenuated in the glycerol-adding group (Figure 1h), which may be imputed to the inhibitory influence of glycerol on RPA. In addition, the obvious phenomenon of phase separation was observed when the RPA reagent was added to the mixtures of glycerol and Cas12a (Figure S3). Taken together, the above experiment data corroborated our speculation that the enhanced detection efficiency was attributed to the phase separation of RPA and the CRISPR/Cas12a system during the initial phase of the RPA reaction caused by the glycerol viscosity. Based on this, we established a glycerol-enhanced one-pot RPA-CRISPR/Cas12a method (Figure 1i). To implement better testing performance, the key parameters of this method including the concentrations of RPA primers and Cas12a, the reaction buffer in the CRISPR

https://doi.org/10.1021/acs.analchem.2c00616
Anal. Chem. 2022, 94, 8277−8284

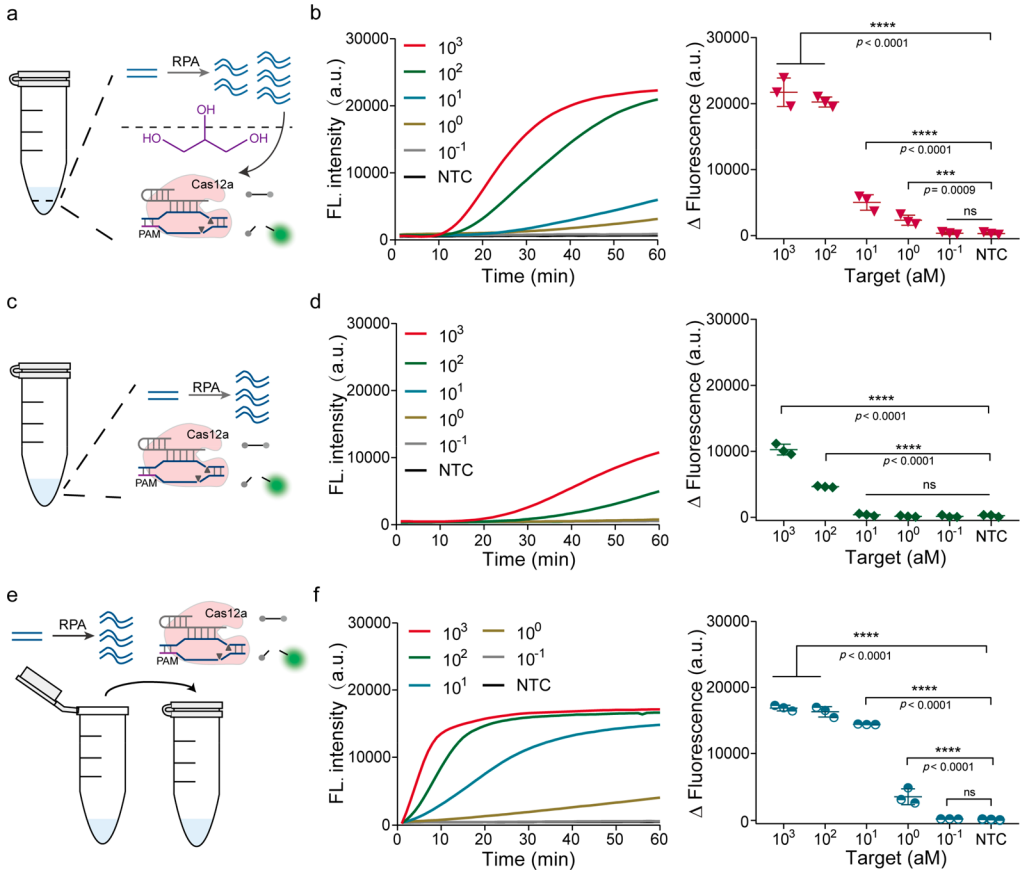


Figure 2. Evaluation of the analytical sensitivity of glycerol-enhanced one-pot RPA-CRISPR/Cas12a method. (a) Schematic of glycerol-enhanced one-pot RPA-CRISPR/Cas12a method. (b) Analytical sensitivity of glycerol-enhanced one-pot RPA-CRISPR/Cas12a method. (c) Schematic of glycerol-free one-pot RPA-CRISPR/Cas12a method. (d) Analytical sensitivity of glycerol-free one-pot RPA-CRISPR/Cas12a method. (e) Schematic of canonical two-step method. (f) Analytical sensitivity of canonical two-step method. The real-time fluorescence curves are shown in the left penal, and end point fluorescence is shown in the right panel. Error bars represent the mean ± standard deviation (SD) from three replicates. NTC represents no target control. *, $P < 0.05$; **, $P < 0.01$; ***, $P < 0.001$; ****, $P < 0.0001$; ns, not significant.

system, and the reaction temperature were optimized (Figure S4).

Evaluation of the Analytical Sensitivity of Glycerol-Enhanced One-Pot RPA-CRISPR/Cas12a Method. In the assay, we drew the conclusion that glycerol dramatically accelerated the detection efficiency of the one-pot RPA-CRISPR system. Here the analytical sensitivity was further confirmed by using gradient diluted ASFV DNA (Figure 2a) and it was found that the limit of detection unequivocally reached 10^0 aM (Figure 2b). We compared it with the sensitivity of the glycerol-free one-pot method (Figure 2c). The result suggested that the sensitivity of the glycerol-enhanced one-pot method was sufficiently 100 times higher than that of the glycerol-free version, whose detection limit barely attained 10^2 aM (Figure 2d). We further wondered whether its sensitivity can be comparable to that of the canonical two-step assay, and the latter sensitivity was determined (Figure 2e). It was demonstrated that the detection limit of the two-step method was also 10^0 aM (Figure 2f). That is, the glycerol-enhanced one-pot method implemented preeminent analytical sensitivity that was identical with that of the two-step method.

Glycerol-Enhanced One-Pot RPA-CRISPR/Cas12a Method for Detection of African Swine Fever Virus (ASFV). Upon developing an ultrasensitive, rapid, and simple one-pot nucleic acid assay method, we harnessed it for detecting African swine fever (ASF) to estimate its assay application (Figure 3a). ASFV infects domestic pigs and wild boars with a mortality rate up to 100%.[41,42] So far, the most effective way to prevent this disease is to adopt rapid, accurate, and sensitive diagnostic methods.

The capsid protein *P72* gene of ASFV was chose as the testing genetic locus (Figure S5). Above all, the sensitivity for assaying the *P72* gene was appraised using the samples with different cycle threshold (Ct) values confirmed by the standard PCR kit. As demonstrated in Figure 3b, the method could test the ASFV samples with a Ct value as low as 35.93. Then, we compared its detection limit with those of the glycerol-free one-pot method and the two-step method. It was found that the limit of detection in the two-step assay was consistent with that of our method, while the glycerol-free one-pot method merely checked out the target of Ct 29.63, highlighting the excellent sensitivity and robust testing performance in our method (Figure 3c and Figure S6). Subsequently, the specificity for ASFV detection was estimated by choosing the DNAs extracted from four kinds of swine susceptible pathogenic bacteria (pseudorabies virus (PRV), *Haemophilus parasuis* (HPS), porcine circovirus (PCV), and *Streptococcus suis* (SS)) as interferences. The obvious increment in the fluorescence signal was only aroused by the existence of ASFV, illuminating no cross-reactivity with DNA from other pathogenic bacteria (Figure 3d). Next, to further inspect its

https://doi.org/10.1021/acs.analchem.2c00616
Anal. Chem. 2022, 94, 8277−8284

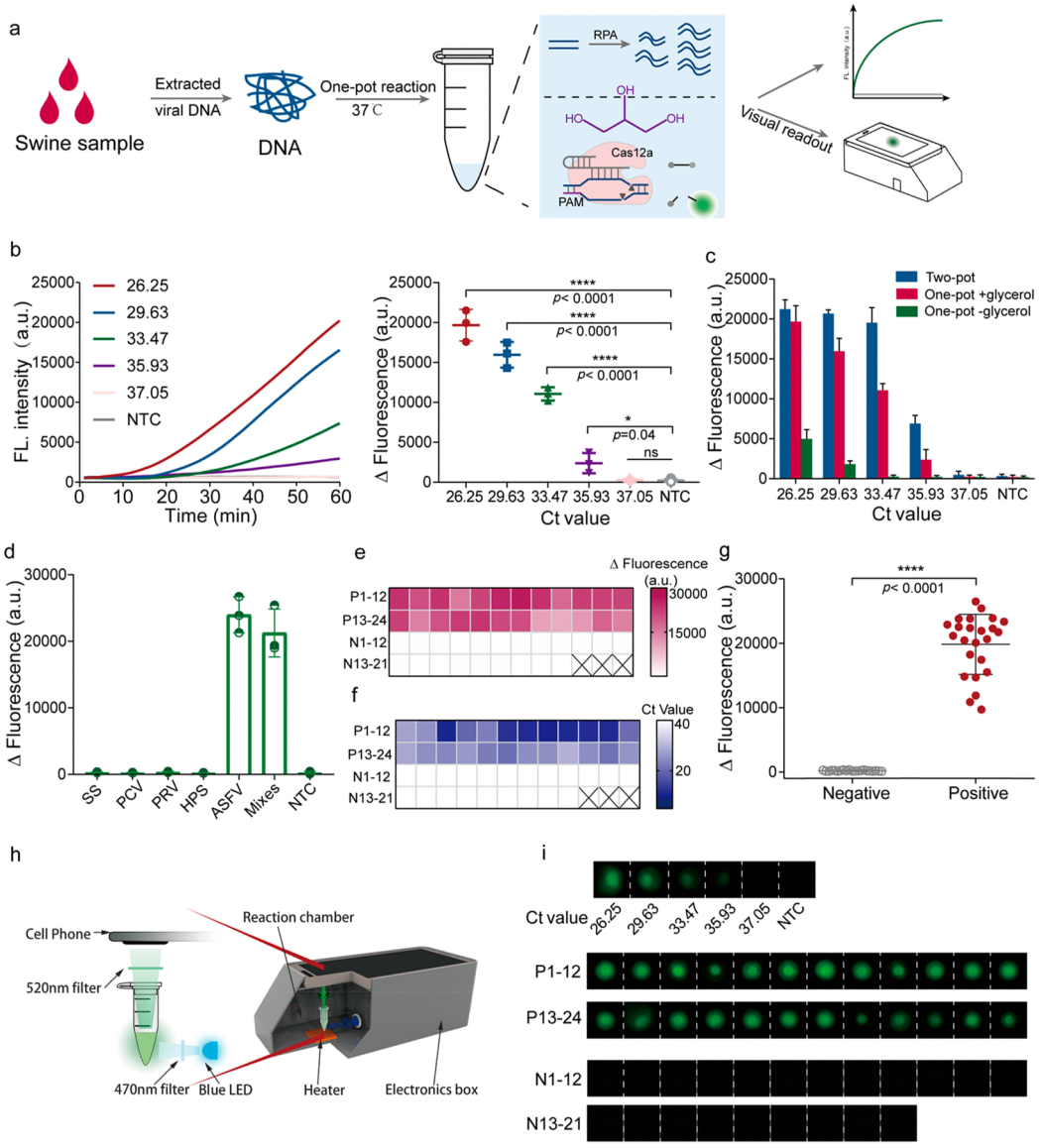


Figure 3. African swine fever virus (ASFV) assay by glycerol-enhanced one-pot RPA-CRISPR/Cas12a method. (a) Schematic diagram of the workflow of ASFV detection in swine serum samples. (b) Evaluation of analytical sensitivity for ASFV detection. (c) Comparison of sensitivity among three assay methods. (d) Evaluation of selectivity for ASFV detection. "Mixes" represents the DNA mixtures including PRV, PCV, SS, HPS, and ASFV. (e, f) Heat map showing the results of ASFV detection in 45 suspected swine serum samples using glycerol-enhanced one-pot RPA-CRISPR/Cas12a method (e) and qPCR (f). (g) Scatter plot showing fluorescence intensity of 24 negative samples and 21 positive samples (two-tailed Student's *t* test). (h) Schematic of detection device showing LED transilluminators, excitation filters, and emission filters for visualization fluorescence signals and a smartphone for image capture. (i) Sensitivity evaluation by imaging signal using the POC testing device in (h) (top panel). End point (60 min) signal images captured by smartphone for ASFV detection in 45 clinical samples (bottom panel).

practical application, the 45 ASFV serum samples were assayed. As expected, the method explicitly identified 24 infected samples and 21 healthy samples from 45 suspected swine serum samples (Figure 3e,g and Figure S7), which exhibited 100% consistency with the gold standard method (RT-PCR) (Figure 3f; Figure S8 and Table S3). In a word, this method possessed 100% accuracy and 100% selectivity in the clinical application of ASFV detection.

For simplifying the signal readout and obviating the employment of a sophisticated instrument, we designed a handheld device based on fluorescence imaging of smartphones with a heating function. In this device, the ssDNA reporting probe was excited by a blue LED light source, and the fluorescence signal intensity was monitored by the smartphone integrated device (Figure 3h and Figure S9). That is, the real-time fluorescence signal in the tube can be directly observed by the naked eye. With the support of this device, it could be completed in one step from the addition of samples to readout results. To confirm the limit of detection (LOD) of the signal readout from the visual device, the ASFV DNA in Figure 3b was tested and the fluorescence signals were collected after 60 min of incubation. We found the analytical sensitivity was identical with that of the standard fluorescence detector (Figure 3i). Next, the device was leveraged to assay clinical samples in Figure 3e, and the results presented 100% consistency with the standard fluorescence detectors (Figure 3i). These above experimental data explicated that, integrating with the portable device, our assay accomplished rapid and

https://doi.org/10.1021/acs.analchem.2c00616
Anal. Chem. 2022, 94, 8277−8284

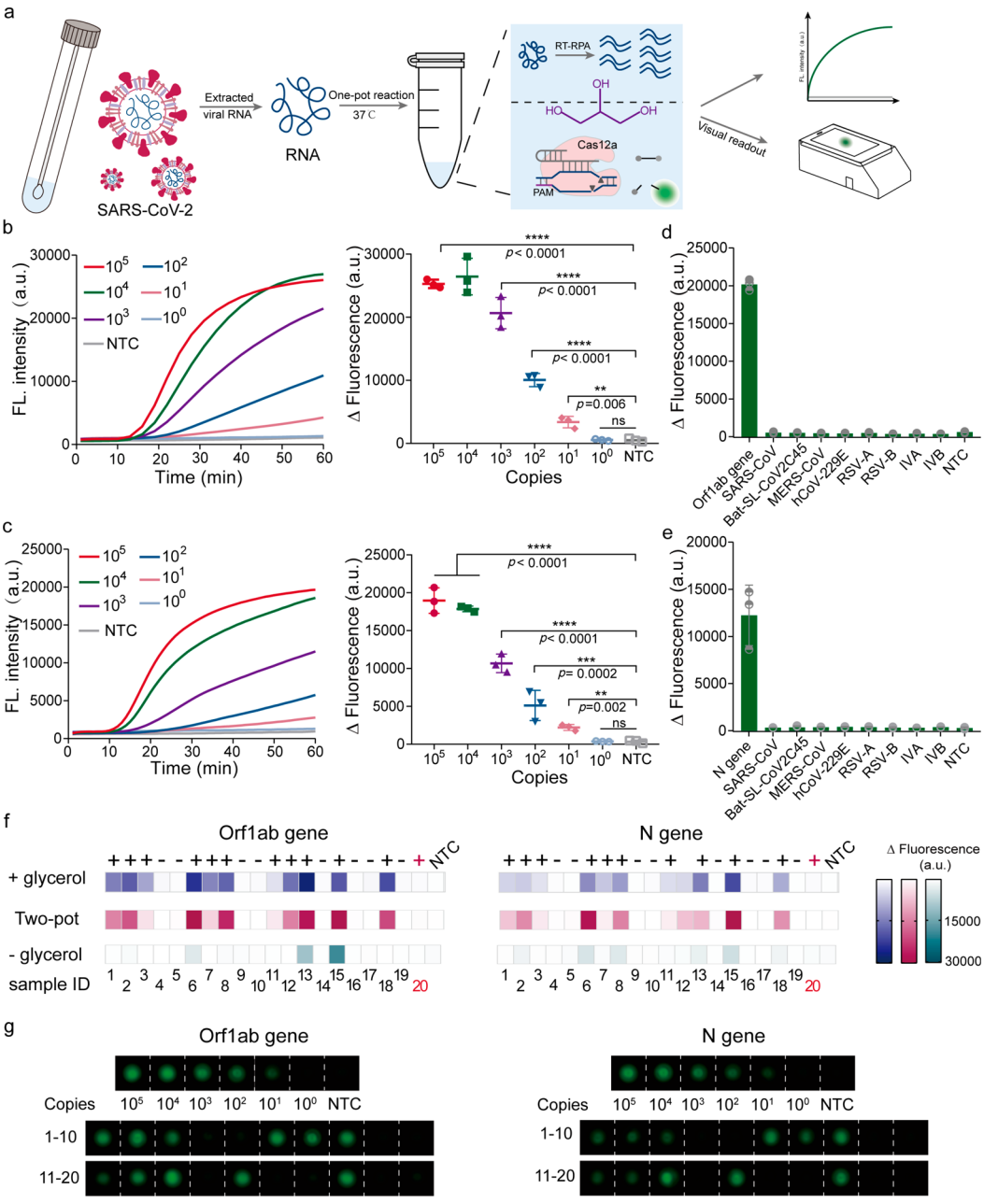


Figure 4. SARS-CoV-2 detection using glycerol-enhanced one-pot RPA-CRISPR/Cas12a method. (a) Schematic diagram of the workflow of SARS-CoV-2 detection in clinical samples. (b, c) Determination of LODs for *Orf1ab* gene (b) and *N* gene (c) in SARS-CoV-2 in our method, using serially diluted in vitro synthesized SARS-CoV-2 RNA standards. Real-time fluorescence curves are shown in left panels, and end point fluorescent signals are shown in right panels. (d, e) Specificity analysis of SARS-CoV-2 RNA. (f) Heat map showing the results of *Orf1ab* gene (left panel) and *N* gene (right panel) detection in 20 suspected COVID-19 clinical samples using three assay methods, respectively. The "+" and "−" represent the positive sample and the negative sample confirmed by RT-PCR, respectively. The number "20" in red means sample 20 cannot be accurately detected in 20 nasopharyngeal swab specimens. (g) Signal images captured by smartphone based on the detection of SARS-CoV-2 with different copies (top panel) and 20 suspected COVID-19 clinical samples (bottom panel). Error bars represent mean ± standard error of the mean (SEM) from three different individual experiments. NTC represents no-template control. **, $P < 0.01$; ***, $P < 0.001$; ****, $P < 0.0001$.

simple nucleic acid detection, which provides a simple, reliable, and easy-to-use method for molecular diagnosis in the field.

SARS-CoV-2 Assay Using Glycerol-Enhanced One-Pot RPA-CRISPR/Cas12a Method. The glycerol-enhanced one-pot method appeared to possess splendid sensitivity, specificity, and accuracy in assaying the DNA virus ASFV. To further prove its versatility, SARS-CoV-2 was taken as an illustration to evaluate the assay performance against RNA viruses (Figure 4a). Severe acute respiratory syndrome coronavirus 2 (SARS-CoV-2), the novel RNA virus responsible for the COVID-19 pandemic, poses a severe threat to global human health and global economic stability.[43,44] The effective way to control the pandemic of COVID-19 is large-scale population screening. It calls for exploiting a highly convenient, sensitive, and accurate SARS-CoV-2 detection method.

The open reading frame 1ab gene (*Orf1ab* gene) and nucleocapsid protein gene (*N* gene) were selected as the gene loci for SARS-CoV-2 testing (Figure S10). With the use of

https://doi.org/10.1021/acs.analchem.2c00616
Anal. Chem. 2022, 94, 8277−8284

serial diluted SARS-CoV-2 standard RNA, the sensitivity for assaying two genes was validated and the detection limit of 10 copies of both genes was acquired (Figure 4b,c). To testify to its specificity, we performed this method using RNA input from other coronaviruses (SARS-CoV, Bat-SL-CoV2C45, MERS-CoV, and hCoV-229E) and some human respiratory viruses (RSV-A, RSV-B, IVA, and IVB). The results showed that there was no cross-reactivity with other RNA viruses in both gene assays (Figure 4d,e).

Next, in order to examine its testing performance in the clinical application for SARS-CoV-2 assay, 20 nasopharyngeal swab clinical samples identified by RT-PCR (12 positive samples and 8 negative samples) were tested (Figure S11 and Table S4). For both genes, our method was capable of accurately determining 8 negative samples and 11 positive samples from 20 samples, except for sample 20 (*Orf1ab* gene Ct 36.10, *N* gene Ct 37.14) (Figure 4f and Figure S12). For comparison, 20 clinical samples were also detected through the glycerol-free one-pot method and the two-step method, respectively. The results manifested that, in the two-step assay, concordant results with our method were obtained, while only four positive samples of *O* gene and six positive samples of *N* gene were checked by the glycerol-free one-pot method (Figure 4f and Figures S13 and S14). The results further indicated that, in clinical practice, our method possessed consistent assay performance with that of the two-step model. After that, the LOD of SARS-CoV-2 assays using visualization equipment was measured, and we found the fluorescence signal of 10 copies could be distinctly observed by the naked eye (Figure 4g). Then, the device was exploited to detect 20 clinical samples (Figure 4f), and the results corresponded with those of the standard fluorescence detector (Figure 4g). Overall, these results meant that this method had great application prospects in point-of-care screening of SARS-CoV-2.

CONCLUSION

In the study, based on the finding that glycerol delayed the fusion of the Cas12a detection system and the RPA amplification system in a tube on account of its viscosity, we developed an ultrasensitive, simple one-pot RPA-CRISPR/Cas12a nucleic acid testing method. Compared with some one-pot methods that called for introducing more crRNAs[34] or thiophosphate modification primers[45] to accomplish high-sensitivity detection, it just needs to simply add low-cost glycerol to the one-pot system. The addition of glycerol elevates the sensitivity of one-pot detection by 2 orders of magnitude and achieves consistent sensitivity with the canonical two-step model. In addition, all the components of isothermal amplification and CRISPR/Cas12a detection are integrated into a single reaction system, eliminating the demand for additional steps including centrifugation,[27−29] uncap and product transfer,[46,47] and so on. To render our method deployable on-site, a portable handheld device was fabricated to readout assay results visually, which fulfilled sample to result without the employment of laboratorial incubation or signal readout instruments. As a proof of concept, this method has been successfully harnessed for the assay of the DNA virus ASFV and the RNA virus SARS-CoV-2. It also can be utilized for precise testing of other highly infectious pathogens.

Of course, we also expect additional improvements in this one-pot method. For example, in order to shorten the response time of sample to result, a sample treatment scheme without nucleic acid extraction could be considered. Besides, to accomplish the procedure of sample in to result out, a smartphone app could be exploited to facilitate subsequent data processing. Through these improvements, the current assay method can be transformed totally into a mature and extensively available POC platform.

In conclusion, the glycerol-enhanced one-pot RPA-CRISPR/Cas12a method reveals substantial superior qualities, including high versatility, ultrahigh sensitivity, independence from sophisticated instruments, splendid accuracy, and ease of use. It provides a direction toward constructing a user-friendly, low-cost point-of-test detection platform and holds great potential for large-scale population screening and accurate diagnosis for COVID-19 and other pandemics.

ASSOCIATED CONTENT

Supporting Information

The Supporting Information is available free of charge at https://pubs.acs.org/doi/10.1021/acs.analchem.2c00616.

Additional experimental details, materials, and methods, including sequence information and supplemental results (PDF)

AUTHOR INFORMATION

Corresponding Authors

Xiaoming Zhou − *School of Life Sciences, South China Normal University, Guangzhou 510631, China; MOE Key laboratory of Laser Life Science & Guangdong Provincial Key Laboratory of Laser Life Science, College of Biophotonics, South China Normal University, Guangzhou 510631, China*; orcid.org/0000-0001-5597-4804; Email: zhouxm@scnu.edu.cn

Yongzhong Jiang − *Hubei Provincial Center for Disease Control and Prevention, Wuhan 430079, China*; Email: 575652423@qq.com

Authors

Mei Lin − *School of Life Sciences, South China Normal University, Guangzhou 510631, China*

Huahua Yue − *School of Life Sciences, South China Normal University, Guangzhou 510631, China*

Tian Tian − *School of Life Sciences, South China Normal University, Guangzhou 510631, China*

Erhu Xiong − *School of Life Sciences, South China Normal University, Guangzhou 510631, China*; orcid.org/0000-0002-9085-1858

Debin Zhu − *Guangzhou Key Laboratory of analytical Chemistry for Biomedicine, School of Chemistry, South China Normal University, Guangzhou 510006, China*

Complete contact information is available at: https://pubs.acs.org/10.1021/acs.analchem.2c00616

Notes

The authors declare no competing financial interest.

ACKNOWLEDGMENTS

This work was supported by the National Natural Science Foundation of China (32150019, 91959128, and 21874049), the Key Research and Development Plan of Hubei Province (2020BCA090), and the Guangdong Basic and Applied Basic Research Foundation (2021A1515220164).

REFERENCES

(1) Pardee, K.; Green, A. A.; Takahashi, M. K.; Braff, D.; Lambert, G.; Lee, J. W.; Ferrante, T.; Ma, D.; Donghia, N.; Fan, M.; Daringer, N. M.; Bosch, I.; Dudley, D. M.; O'Connor, D. H.; Gehrke, L.; Collins, J. J. *Cell* **2016**, *165* (5), 1255−1266.

(2) Du, Y.; Dong, S. *Anal. Chem.* **2017**, *89* (1), 189−215.

(3) Li, M.; Yin, F.; Song, L.; Mao, X.; Li, F.; Fan, C.; Zuo, X.; Xia, Q. *Chem. Rev.* **2021**, *121* (17), 10469−10558.

(4) Liu, G.; Lin, Q.; Jin, S.; Gao, C. *Mol. Cell* **2022**, *82* (2), 333−347.

(5) Kaminski, M. M.; Abudayyeh, O. O.; Gootenberg, J. S.; Zhang, F.; Collins, J. J. *Nat. Biomed Eng.* **2021**, *5* (7), 643−656.

(6) Anzalone, A. V.; Koblan, L. W.; Liu, D. R. *Nat. Biotechnol.* **2020**, *38* (7), 824−844.

(7) Li, S. Y.; Cheng, Q. X.; Liu, J. K.; Nie, X. Q.; Zhao, G. P.; Wang, J. *Cell Res.* **2018**, *28* (4), 491−493.

(8) Chen, J. S.; Ma, E. B.; Harrington, L. B.; Da Costa, M.; Tian, X. R.; Palefsky, J. M.; Doudna, J. A. *Science* **2018**, *360* (6387), 436.

(9) East-Seletsky, A.; O'Connell, M. R.; Knight, S. C.; Burstein, D.; Cate, J. H.; Tjian, R.; Doudna, J. A. *Nature* **2016**, *538* (7624), 270−273.

(10) Yang, H.; Gao, P.; Rajashankar, K. R.; Patel, D. J. *Cell* **2016**, *167* (7), 1814−1828.

(11) Harrington, L. B.; Burstein, D.; Chen, J. S.; Paez-Espino, D.; Ma, E.; Witte, I. P.; Cofsky, J. C.; Kyrpides, N. C.; Banfield, J. F.; Doudna, J. A. *Science* **2018**, *362* (6416), 839−842.

(12) Chertow, D. S. *Science* **2018**, *360* (6387), 381−382.

(13) Li, Y.; Li, S.; Wang, J.; Liu, G. *Trends Biotechnol* **2019**, *37* (7), 730−743.

(14) Fozouni, P.; Son, S.; Diaz de Leon Derby, M.; Knott, G. J.; Gray, C. N.; D'Ambrosio, M. V.; Zhao, C.; Switz, N. A.; Kumar, G. R.; Stephens, S. I.; Boehm, D.; Tsou, C. L.; Shu, J.; Bhuiya, A.; Armstrong, M.; Harris, A. R.; Chen, P. Y.; Osterloh, J. M.; Meyer-Franke, A.; Joehnk, B.; Walcott, K.; Sil, A.; Langelier, C.; Pollard, K. S.; Crawford, E. D.; Puschnik, A. S.; Phelps, M.; Kistler, A.; DeRisi, J. L.; Doudna, J. A.; Fletcher, D. A.; Ott, M. *Cell* **2021**, *184* (2), 323−333.

(15) Zhang, J.; Lv, H.; Li, L.; Chen, M.; Gu, D.; Wang, J.; Xu, Y. *Front Microbiol* **2021**, *12*, 751408.

(16) Feng, W.; Newbigging, A. M.; Tao, J.; Cao, Y.; Peng, H.; Le, C.; Wu, J.; Pang, B.; Li, J.; Tyrrell, D. L.; Zhang, H.; Le, X. C. *Chem. Sci.* **2021**, *12* (13), 4683−4698.

(17) Notomi, T.; Okayama, H.; Masubuchi, H.; Yonekawa, T.; Watanabe, K.; Amino, N.; Hase, T. *Nucleic Acids Res.* **2000**, *28* (12), No. e63.

(18) Piepenburg, O.; Williams, C. H.; Stemple, D. L.; Armes, N. A. *PLoS Biol.* **2006**, *4* (7), No. e204.

(19) Lee, R. A.; Puig, H.; Nguyen, P. Q.; Angenent-Mari, N. M.; Donghia, N. M.; McGee, J. P.; Dvorin, J. D.; Klapperich, C. M.; Pollock, N. R.; Collins, J. J. *Proc. Natl. Acad. Sci. U.S.A.* **2020**, *117* (41), 25722−25731.

(20) de Puig, H.; Lee, R. A.; Najjar, D.; Tan, X.; Soenksen, L. R.; Angenent-Mari, N. M.; Donghia, N. M.; Weckman, N. E.; Ory, A.; Ng, C. F.; Nguyen, P. Q.; Mao, A. S.; Ferrante, T. C.; Lansberry, G.; Sallum, H.; Niemi, J.; Collins, J. J. *Sci. Adv.* **2021**, *7*, No. eabh2944.

(21) Kellner, M. J.; Koob, J. G.; Gootenberg, J. S.; Abudayyeh, O. O.; Zhang, F. *Nat. Protoc* **2019**, *14* (10), 2986−3012.

(22) Li, S. Y.; Cheng, Q. X.; Wang, J. M.; Li, X. Y.; Zhang, Z. L.; Gao, S.; Cao, R. B.; Zhao, G. P.; Wang, J. *Cell Discovery* **2018**, *4*, 20.

(23) Gootenberg, J. S.; Abudayyeh, O. O.; Lee, J. W.; Essletzbichler, P.; Dy, A. J.; Joung, J.; Verdine, V.; Donghia, N.; Daringer, N. M.; Freije, C. A.; Myhrvold, C.; Bhattacharyya, R. P.; Livny, J.; Regev, A.; Koonin, E. V.; Hung, D. T.; Sabeti, P. C.; Collins, J. J.; Zhang, F. *Science* **2017**, *356* (6336), 438−442.

(24) Gootenberg, J. S.; Abudayyeh, O. O.; Kellner, M. J.; Joung, J.; Collins, J. J.; Zhang, F. *Science* **2018**, *360* (6387), 439−444.

(25) Li, L.; Li, S.; Wu, N.; Wu, J.; Wang, G.; Zhao, G.; Wang, J. *ACS Synth. Biol.* **2019**, *8* (10), 2228−2237.

(26) Zetsche, B.; Gootenberg, J. S.; Abudayyeh, O. O.; Slaymaker, I. M.; Makarova, K. S.; Essletzbichler, P.; Volz, S. E.; Joung, J.; van der Oost, J.; Regev, A.; Koonin, E. V.; Zhang, F. *Cell* **2015**, *163* (3), 759−71.

(27) Wang, B.; Wang, R.; Wang, D.; Wu, J.; Li, J.; Wang, J.; Liu, H.; Wang, Y. *Anal. Chem.* **2019**, *91* (19), 12156−12161.

(28) Pang, B.; Xu, J.; Liu, Y.; Peng, H.; Feng, W.; Cao, Y.; Wu, J.; Xiao, H.; Pabbaraju, K.; Tipples, G.; Joyce, M. A.; Saffran, H. A.; Tyrrell, D. L.; Zhang, H.; Le, X. C. *Anal. Chem.* **2020**, *92* (24), 16204−16212.

(29) Wang, Y.; Ke, Y.; Liu, W.; Sun, Y.; Ding, X. *ACS Sens* **2020**, *5* (5), 1427−1435.

(30) Yin, K.; Ding, X.; Li, Z.; Zhao, H.; Cooper, K.; Liu, C. *Anal. Chem.* **2020**, *92* (12), 8561−8568.

(31) Ramachandran, A.; Huyke, D. A.; Sharma, E.; Sahoo, M. K.; Huang, C.; Banaei, N.; Pinsky, B. A.; Santiago, J. G. *PANS* **2020**, *117* (47), 29518−29525.

(32) Li, Z.; Ding, X.; Yin, K.; Avery, L.; Ballesteros, E.; Liu, C. *Biosens Bioelectron* **2022**, *199*, 113865.

(33) Chen, Y.; Mei, Y.; Zhao, X.; Jiang, X. *Anal. Chem.* **2020**, *92* (21), 14846−14852.

(34) Ding, X.; Yin, K.; Li, Z.; Lalla, R. V.; Ballesteros, E.; Sfeir, M. M.; Liu, C. *Nat. Commun.* **2020**, *11* (1), 4711.

(35) Feng, W.; Peng, H.; Xu, J.; Liu, Y.; Pabbaraju, K.; Tipples, G.; Joyce, M. A.; Saffran, H. A.; Tyrrell, D. L.; Babiuk, S.; Zhang, H.; Le, X. C. *Anal. Chem.* **2021**, *93* (37), 12808−12816.

(36) Zeng, Z.; Yan, H.; Zheng, X.; Hu, G.; Chen, Y.; Mei, D. *Life Sci. J.* **2006**, *3* (1), 67−71.

(37) Henke, W.; Herdel, K.; Jung, K.; Schnorr, D.; Loening, S. A. *Nucleic Acids Res.* **1997**, *25* (19), 3957−8.

(38) Jensen, M. A.; Fukushima, M.; Davis, R. W. *PLoS One* **2010**, *5* (6), No. e11024.

(39) Li, Z.; Zhao, W.; Ma, S.; Li, Z.; Yao, Y.; Fei, T. *Biosens Bioelectron* **2021**, *192*, 113493.

(40) Maturada, P.; Aimorn, H.; Kanokpol, A.; et al. A multiplexed Cas13-based assay with point-of-care attributes for simultaneous COVID-19 diagnosis and variant surveillance. *medRxiv*, March 18, 2022, 2022.03.17.22272589. DOI: 10.1101/2022.03.17.22272589.

(41) Sanchez-Cordon, P. J.; Montoya, M.; Reis, A. L.; Dixon, L. K. *Vet J.* **2018**, *233*, 41−48.

(42) Galindo, I.; Alonso, C. *Viruses* **2017**, *9* (5), 103.

(43) Wang, C.; Horby, P. W.; Hayden, F. G.; Gao, G. F. *Lancet* **2020**, *395* (10223), 470−473.

(44) Zhou, P.; Yang, X. L.; Wang, X. G.; Hu, B.; Zhang, L.; Zhang, W.; Si, H. R.; Zhu, Y.; Li, B.; Huang, C. L.; Chen, H. D.; Chen, J.; Luo, Y.; Guo, H.; Jiang, R. D.; Liu, M. Q.; Chen, Y.; Shen, X. R.; Wang, X.; Zheng, X. S.; Zhao, K.; Chen, Q. J.; Deng, F.; Liu, L. L.; Yan, B.; Zhan, F. X.; Wang, Y. Y.; Xiao, G. F.; Shi, Z. L. *Nature* **2020**, *579* (7798), 270−273.

(45) Gong, J.; Kan, L.; Zhang, X.; He, Y.; Pan, J.; Zhao, L.; Li, Q.; Liu, M.; Tian, J.; Lin, S.; Lu, Z.; Xue, L.; Wang, C.; Tang, G. *Bioact Mater.* **2021**, *6* (12), 4580−4590.

(46) Broughton, J. P.; Deng, X.; Yu, G.; Fasching, C. L.; Servellita, V.; Singh, J.; Miao, X.; Streithorst, J. A.; Granados, A.; Sotomayor-Gonzalez, A.; Zorn, K.; Gopez, A.; Hsu, E.; Gu, W.; Miller, S.; Pan, C. Y.; Guevara, H.; Wadford, D. A.; Chen, J. S.; Chiu, C. Y. *Nat. Biotechnol.* **2020**, *38* (7), 870−874.

(47) Ooi, K. H.; Liu, M. M.; Tay, J. W. D.; Teo, S. Y.; Kaewsapsak, P.; Jin, S.; Lee, C. K.; Hou, J.; Maurer-Stroh, S.; Lin, W.; Yan, B.; Yan, G.; Gao, Y. G.; Tan, M. H. *Nat. Commun.* **2021**, *12* (1), 1739.

https://doi.org/10.1021/acs.analchem.2c00616
Anal. Chem. 2022, 94, 8277−8284